COMPARISONS OF LRO LAMP AND MINI-RF DATASETS WITHIN ANOMALOUS POLAR CRATERS. Angela M. Stickle[1], Dana M. Hurley[1], G. Wesley Patterson[1], J.T.S Cahill[1], Kurt D. Retherford[2], G. Randall Gladstone[2], Thomas K. Greathouse[2], Kathleen E. Mandt[2], Amanda R. Hendrix[3], Anthony Egan[4], David Kaufmann[4] ,Wayne Pryor[5], Paul Feldman[6], Alan Stern[4]; [1]Johns Hopkins University Applied Physics Laboratory, Laurel, MD, 20723, USA, [2]Southwest Research Institute, Space Science & Engineering, San Antonio, TX 78228,[3]Planetary Science Institute, Tucson, AZ 85719,[4]Southwest Research Institute, Boulder CO, [5]Central Arizona College, Coolidge, AZ 85128, [6]Johns Hopkins University, Baltimore MD. (angela.stickle@jhuapl.edu)

Introduction: The permanently shadowed regions (PSRs) at the lunar poles are hypothesized to be excellent traps for volatiles due to their constant darkness and extremely cold temperatures. [e.g., 1-4]; remote sensing data can provide clues as to the nature of these traps. Analysis of Clementine bistatic radar observation of the south polar region of the Moon suggested an enhancement in CPR associated with the crater Shackleton and interpreted as resulting from volumentric scattering of water ice [5]. Neutron data suggests enhanced hydrogen concentrations at high latitudes [6-7]; other remote observations provided evidence of trace amounts of ice or bound OH on the Moon [e.g., 8-9]. Some PSRs show signs of enhanced hydrogen concentrations possibly located within the craters [6-7]. One such area, the PSRs within Cabeus crater near the lunar south pole, was the target of the LCROSS mission. The LCROSS team identified the presence of water ice in the ejecta plume following impact, providing "ground truth" to some of the remotely sensed data [10]. Though water has been observed using multiple data sets and various wavelengths, more work is necessary in order to fully understand the distribution and nature of volatiles on the moon. The suite of instruments onboard LRO provide opportunities to examine signatures of volatiles across different wavelengths to better understand where water ice is located on the Moon and its behavior. Here, we compare data from two instruments onboard LRO, the Miniature Radio Frequency (Mini-RF) radar [11] and the Lyman Alpha Mapping Project (LAMP) far ultraviolet (FUV) imaging spectrograph [12], to examine the possibility of volatiles being trapped in a set of specific PSRs: the anomalous craters identified in Spudis et al. [13].

Mini-RF Data: The Mini-RF instrument flown on LRO is a Synthetic Aperture Radar (SAR) with a hybrid dual-polarimetric architecture. I.e., the radar transmits a circularly polarized signal, and receives orthogonal linear polarizations and their relative phase [14]. The returned information can be represented using the classical Stokes parameters (S_1, S_2, S_3, S_4) [15], which can be used to derive a variety of useful products to characterize the radar scattering properties of the lunar surface. CPR is commonly used in analyses of planetary radar data [16-17] and is given by: CPR = $(S_1-S_4)/(S_1+S_4)$. It is a representation of surface roughness on the order of the radar wavelength (e.g., meter scale features). For example, a specular reflection would result in a CPR of zero, while higher CPR values occur from multiple scattering from double reflectors or the presence of a low-loss medium in the subsurface. In general, fresh craters will exhibit high CPR values in and around the crater rim, where large amounts of wavelength-scale surface roughness is present in the blocky ejecta blankets, impact melt flows, and fallback breccia, and CPR can often be used to identify and analyze properties young lunar crater deposits. Low-loss mediums, such as water-ice will also result in high CPR values.

LAMP Data: The LAMP FUV imaging spectrograph onboard LRO [11] uses UV starlight and Lyman-α skyglow as its primary light source, which allows it to "see" into regions on the moon that are permanently shaded from sunshine or earthshine in search of signatures of water ice. LAMP maps (~240 mpp) of the Lyman-α (119-125 nm), "On"- (130-155 nm) and "Off"- (155-190 nm) band albedo from the first 18 months of data are used here to examine the FUV properties of the lunar surface, and can be especially useful in searching for and diagnosing porosity changes or the presence of water frost at the lunar surface.

Polar Anomalous Craters: Using data from Mini-RF, Spudis et al. [13] identified craters at both lunar poles that exhibited unique CPR characteristics. These craters, 44 at the north pole and 28 at the south pole, exhibit high CPR only in their dark, cold (less than 100K) interiors. Using scattering models, Spudis et al. suggest that these anomonalously-high CPR deposits are consistent with the presence of water ice.

Alternative hypotheses have also been suggested [e.g., 18-19]. By comparing detailed scattering simulations with Mini-SAR and Mini-RF data, Fa et al. [18] conclude that the most important factor influencing CPR values is the radar incident angle. Eke et al. [19] suggest that the enhanced CPR signals within these anomalous craters are largely due to steep sloping crater walls that affect the geometry of the observations. Detailed scattering simulations show that identifying water ice mixed in the lunar regolith may be difficult using CPR alone due to the small contrast of

dielectric permittivity between ice and silicate regolith [18].

Here, the craters identified in [13] are examined in LRO-LAMP data. Comparing these data to Mini-RF observations may provide insights into the presence or lack of water ice in these anomalous regions at the lunar poles.

Preliminary Comparisons: Preliminary examination of LAMP data for the anomalous craters identified by Spudis et al. [13] suggests some differences in surface properties between material inside the crater compared to material outside, but near to, the crater rim. Distributions of the Lyman-α albedo were examined for the material on the floor and walls of each identified crater to compare to an annulus encompassing material outside the crater rim. For the anomalous craters at both poles, the mean Lyman-α albedo is lower inside the crater 40-44% of the time compared to material outside the rim. In contrast, the mean Lyman-α albedo outside the crater is lower than areas within the rim 56% of the time. The average value is taken of the pixels in the entire crater floor and within the annulus outside the crater, beginning at the rim. Figure 1 shows a typical histogram of a small unnamed crater on the floor of Sylvester (4.8 km, 82.7N, 83.6W, Fig 1 top) and Guassian fits to the data. Red is for material outside the crater and green shows the values of the albedo within the crater.

Future Work: Water ice has a diagnostic spectral reflectance signature in the FUV [20], with a strong absorption edge at ~160-180 nm. Areas containing water frost will have a lower Lyman-α albedo, and frost can be identified by examining the ratio of spectra values above and below the 160-180 nm absorption edge [11]. Gladstone et al. [21] reported that LAMP observed the Lyman-α albedo in PSRs to be lower than surrounding areas. These regions correspond well to areas of coldest Diviner temperature [4; 22]. The best explanation for this difference is that the porosity is higher than other areas. Several PSRs show a relative redenning that indicates there is 1–2% water frost intimately mixed within the upper ~200 nm of the regolith [21]. If the anomalous, high radar backscatter is due to water ice in the craters identified by [13], we might expect similar behavior when looking at them in LAMP data. Further examination, including the "On" and "Off"-band ratios within the LAMP data will be used to more fully constrain the possibility of volatiles in these regions, and may be useful in differentiating between the competing hypotheses for the anomalous Mini-RF signatures reported in [13].

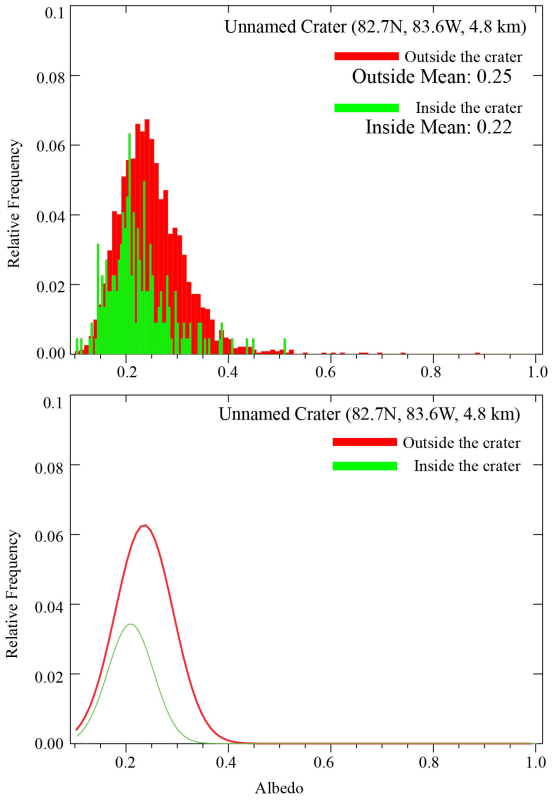

Figure 1. Typical histograms of Lyman-α albedo for an unnamed crater on the floor of Sylvester crater. Green shows the values within the crater and red shows the albedo values outside the crater.

References:[1] Watson et al. (1961) *J. Geophys. Res.* 66, 1598-1600; [2] Arnold, J.R. (1979) *J. Geophys. Res.* 84, 5659-5668; [3] Elphic et al. (2007) *Geophys. Res. Letters* 34(13); [4] Paige et al. (2010) *Science*, 330(6003), 479-482; [5] Spudis, P. et al. (1998), *Space Sci. Res.* 32, 17; [6] Feldman, W. et al. (1998) *Science* 281, 1496-1500; [7] Lawrence et al. (2006) *J. Geophys. Res.* 34, L03201; [8] Pieters, C. et al. 2009 *Science*, 568; [9] Clark, R. (2009) *Science* 326, 562; [10] Colaprete, A. et al. (2010) *Science* 330(6003), 463-468; [11] Gladstone et al. (2009) *Space Sci. Rev.*, 150(1-4), 161-181; [12] Nozette, S. et al (2010) *Space Sci. Rev.*150, 285-302.; [13] Spudis, P. et al. (2013) *J. Geophys. Res.* 118(10), 2016-2029; [14] Raney, R. K. et al. (2011), *Proc. of the IEEE*, 99, 808-823; [15] Stokes (1852), Trans. of the Cambridge Phil. Soc. 9, 399; [16] Campbell et al. (2010), *Icarus*, 208, 565-573; [17] Carter et al. (2012), JGR, 117, E00H09; [18] Fa, W. et al. (2011) *J. Geophys. Res.* 116, E03005; [19] Eke, V. et al. (2014) *Icarus* 241, 66-78; [20] Wagner, J.K. et al. (1987) *Icarus* 69, 14-28; [21] Gladstone, R. et al. (2012) *J. Geophys. Res.* 117(E12), E00H04; [22] Hayne et al. (2015) Icarus.